Journal Pre-proofs

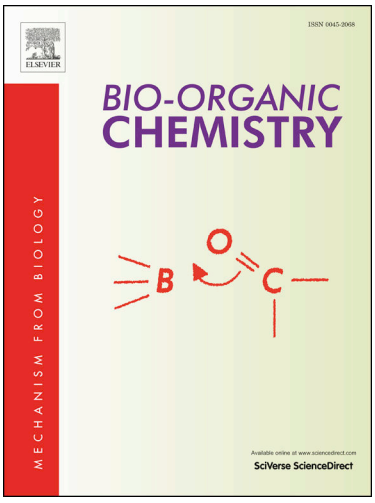

Design, synthesis and evaluation of novel ferulic acid derivatives as multi-target-directed ligands for the treatment of Alzheimer's disease

Jin-Shuai Lan, Rui-Feng Zeng, Xiao-Yi Jiang, Jian-wei Hou, Yun Liu, Zheng-Hao Hu, Hong-Xin Li, Yin Li, Sai-Sai Xie, Yue Ding, Tong Zhang

PII: S0045-2068(19)31262-3
DOI: https://doi.org/10.1016/j.bioorg.2019.103413
Reference: YBIOO 103413

To appear in: *Bioorganic Chemistry*

Received Date: 2 August 2019
Revised Date: 23 October 2019
Accepted Date: 28 October 2019

Please cite this article as: J-S. Lan, R-F. Zeng, X-Y. Jiang, J-w. Hou, Y. Liu, Z-H. Hu, H-X. Li, Y. Li, S-S. Xie, Y. Ding, T. Zhang, Design, synthesis and evaluation of novel ferulic acid derivatives as multi-target-directed ligands for the treatment of Alzheimer's disease, *Bioorganic Chemistry* (2019), doi: https://doi.org/10.1016/j.bioorg.2019.103413

Design, synthesis and evaluation of novel ferulic acid derivatives as multi-target-directed ligands for the treatment of Alzheimer's disease

Jin-Shuai Lan[1,2#], Rui-Feng Zeng[2#], Xiao-Yi Jiang[2], Jian-wei Hou[1], Yun Liu[1], Zheng-Hao Hu[2], Hong-Xin Li[2], Yin Li[4], Sai-Sai Xie[3]*, Yue Ding[1,2]*, Tong Zhang[1,2]*

[1] Experiment Center of Teaching & Learning, Shanghai University of Traditional Chinese Medicine, Shanghai 201203, China;

[2] School of Pharmacy, Shanghai University of Traditional Chinese Medicine, Shanghai 201203, China;

[3] National Pharmaceutical Engineering Center for Solid Preparation in Chinese Herbal Medicine, Jiangxi University of Traditional Chinese Medicine, Nanchang 330006, China;

[4] Hebei Radio & TV University, Shijiazhuang, Hebei 050080, China.

[*] Corresponding author: Sai-Sai Xie; Yue Ding; Tong Zhang

[*] E-mail: xiesaisainanchang@hotmail.com(S-S X); dingyue-2001@hotmail.com (YD); zhangtongshutcm@hotmail.com (TZ)

[#] These authors contributed equally to this work.

Abstract

A series of new ferulic acid derivatives were designed, synthesized and evaluated as multi-target inhibitors against Alzheimer's disease. *In vitro* studies indicated that most compounds showed significant potency to inhibit self-induced *β*-amyloid (A*β*) aggregation and acetylcholinesterase (AChE), and had good antioxidant activity. Specifically, compound **4g** exhibited the potent ability to inhibit cholinesterase (ChE) (IC_{50}, 19.7 nM for *h*AChE and 0.66 μM for *h*BuChE) and the good A*β* aggregation inhibition (49.2% at 20 μM), and it was also a good antioxidant (1.26 trolox equivalents). Kinetic and molecular modeling studies showed that compound **4g** was a mixed-type inhibitor, which could interact simultaneously with the catalytic anionic site (CAS) and the peripheral anionic site (PAS) of AChE. Moreover, compound **4g** could remarkably increase PC12 cells viability in hydrogen peroxide–induced oxidative cell damage and A*β*-induced cell damage. Finally, compound **4g** had good ability to cross the BBB using the PAMPA−BBB assay. These results suggested that compound **4g** was a promising multifunctional ChE inhibitor for the further investigation.

Keywords

Ferulic acid deriveatives; Alzheimer's disease; cholinesterase; A*β* (1-42) aggregation; multi-target-directed ligands; molecular docking.

Abbreviations

AD, Alzheimer's disease; NMDA, N-methyl-Daspartate; AChEs/BChEs, acetylcholinesterase/butyrylcholinesterase; Ach/Buch, acetylcholine/butyrylcholine; MTDLs, multi-target-directed ligands; FA, Ferulic acid; BBB, blood-brain barrier; CAS, catalytic active site; PAS, peripheral anionic site; MTT, Methyl thiazolyl tetrazolium; ADME, absorption, distribution, metabolism and excretion; tPSA, topological polar surface area; CNS, central nervous system; PAMPA, parallel artificial membrane permeation assay.

1. Introduction

Alzheimer's disease (AD), a neurodegenerative, extensive and chronic disease, is clinically described as behavioral disturbances, continuous deterioration of remembrance, studying and cognitive functions [1,2]. To date, there were appraised 46 million people breathing with presenile dementia over the world. Unfortunately, the sum was predicted to approach 131.5 million till 2050 [3]. AD also induced a great amount of economic loss, which was evaluated to cost US $818 billion on senile psychosis in 2018 and the number will rise to 2 trillion dollar before 2030 [4]. Though the scientific characters of AD have been identified for more than 100 years, the therapy of AD is not known owning to its complicated pathogenesis [5]. Significant evidences have revealed that AD is a multifactorial syndrome originated from a composite array of neurochemical ingredient, involving the dearth of synaptic acetylcholine, dyshomeostasis of biometals, the deposition of neurotoxic *β*-amyloid (A*β*) peptide, oxidative stress, the infection of neurons and so on [6,7]. Up to date, the present clinical treatment for presenile dementia is relieving the symptomatic aspects. There were four kinds of drugs approved by the FDA including one N-methyl-Daspartate (NMDA) receptor antagonist, memantine and three acetylcholinesterase inhibitors (AChEs) including rivastigmine, donepezil and galantamine [8]. But sadly, these medicines could only promote memory and cognitive function to a positive level, and they could not prohibit, halt or reverse the developing of AD. Contemporary studies improved that the ratio of butyrylcholinesterase (BuChE)/AChE gradually rose from 0.2 to 11.0 in certain parts of the brain while AD developing. Besides, AChE and BuChE perform similar roles in cholinergic signaling, and BuChE could hydrolyze acetylcholine (ACh) and reimburse for AChE when the level of ACh are depleted [9,10]. Therefore, the drug with both AChE and BuChE inhibitions could better ensure the therapy.

What's more, the production and aggregation of A*β*, chiefly for the subtype of A*β* (1-40) and A*β* (1-42), could endlessly cause neurodegeneration and lead AD patients to neuronal dysfunction at last. So the inhibition of the production and accumulation of A*β* in brain was recognized as a possible target for AD therapy [11,12]. Besides, the progressive aggregation of A*β* is usually attached to oxidative stress, which attends to

be a considerable determinant in AD pathogenesis and progression. And the oxidative damage marked by nitration, reactive carbonyls, lipid peroxidation and nucleic acid oxidation is raised in frail neurons of AD [13,14]. So the protection of neuronal cells from oxidative damage could probably limit the process of AD.

Considering the complex pathogenesis and progression of AD, the therapy targets on a single path might be insufficient. Thus, based on the multi-target-directed ligands (MTDLs) paradigm, the design of multi-target compounds against AD was proposed as a more efficient therapeutic strategy [15-21].

Ferulic acid (4-hydroxy-3-methoxy cinnamic acid, FA) is firstly extracted form Ferula foetida, and widely distribute in kinds of plants. FA is a nature antioxidant and anti-inflammatory compound, and could also act as disaggregating agents of Aβ. Due to the affirmative efficacy and low side-effects of FA, it was recognized as a potential resistant or remedial drug for AD treatment [22]. Nonetheless, FA as an anti-AD drug used in clinic was limited owning to its low bioavailability and poor blood–brain transport. Thus, designing novel FA derivatives based on MTDLs is meaningful for anti-AD [23-28]. As is well-known, AP2238 (**2**), whose pharmacophore was proved to be the benzylamino group, was a highly selective AChE inhibitor for AD treatment, but it displayed poor inhibition on BuChE with IC_{50} value of 48.9 μM [29]. Furthermore, Rivastigmine (**3**), marketed by Novartis as Exelon, is a carbamate pseudo-irreversible AChE inhibitor, which exhibits high selectivity in the hippocampus and cortex of brain, and interferes both AChE and BuChE [30]. However, Rivastigmine can only benefit to simple improvement in cognition, cannot reverse the progression of AD. Considering the mentioned reasons, we planned to combine the FA, the benzylamino group and the carbamyl group with different lengths as a multi-target molecule (Fig. 1). The FA derivatives may simultaneously have the antioxidant activity, ChE inhibitory activity and neuroprotective properties.

Continuing our works on treatment of AD [31-34], a novel series of FA derivatives were constructed based on MTDLs (Fig. 1). They were synthesized and investigated as the multifunctional compounds against AD, containing the inhibitory effects on AChE

and BuChE, protection of antioxidant damage, inhibition of the Aβ aggregation, the capability of crossing blood-brain barrier (BBB) and prevention from H_2O_2-induced and Aβ-induced PC12 cell injury *in vitro*. Finally, the structure-activity relationships of the novel FA derivatives were summarized and molecular modeling studies were also executed to achieve the binding mode.

2. Results and Discussion

2.1 Chemistry

The synthesis of target compounds **4** were shown in scheme 1 with good yields (50-70%). Firstly, the FA derivatives **1** were purchased and pretreated in acetone solutions with Et_3N at 50 °C, and then treated with 1,2-dibromoethane, 1,3-dibromopropane, 1,4-dibromobutane, 1,5-dibromopentane or 1,8-dibromooctane to form the necessary intermediates **2** [35]. Next, compounds **2** were mixed with secondary amines **3** and anhydrous K_2CO_3 in dry acetonitrile at 80 °C to obtain the compounds **4**. At last, the target products were clarified by chromatography, and the structures were confirmed by analytical and spectroscopic data.

2.2 Effect of ChE inhibition activity.

To evaluate the multi-potential function of the new FA derivatives (compounds **4a–o**), we firstly measured their inhibition on both *eq*BuChE (equine serum) and *ee*AChE (electric eel) based on the Ellman's method [36]. FA and Donepezil were applied as standard compounds for comparison. The selectivity index and comparable IC_{50} values of ChEs were exhibited in Table 1. The target compounds exhibited wide inhibitory activities toward *ee*AChE with IC_{50} ranging from 0.055 μM to 42.26 μM, and moderate inhibitory activities towards *eq*BuChE. These results implied that these FA derivatives performed as dual inhibitors of both *ee*AChE and *eq*BuChE, and every target compounds was more efficient than FA on ChEs inhibition. Among the synthesized FA derivatives, compound **4h** (IC_{50} = 0.055 μM) displayed the best inhibitory potency for *ee*AChE, while compound **4b** (IC_{50} = 0.84 μM) exhibited the most potent inhibitory

activity for *eq*BuChE.

First of all, to select the suitable linker lengths between FA and amide groups for ChEs inhibition, compounds **4a–e** with various alkyl chains were investigated. The inhibitory activities for *ee*AChE (in Table 1) changed obviously when the length of the alkyl chains of compounds **4a–e** was altered from 2 to 8. And compound **4d** with five carbon spacers connecting FA with the benzylamino group, had a better *ee*AChE inhibitory activity than the other compounds. Interestingly, similar regularity was also suitable to the inhibition of *eq*BuChE. The results above indicated that five carbon atoms between the two anchoring group was the suitable linker length for the inhibition of ChEs [37]. Next, to further promote the ChEs inhibition of the FA derivatives, we investigated different substituents with various electronic properties and sizes (H, OCH_3, OH and NO_2) on the benzene ring of FA. The results of compounds **4d** and **4f-h** on *ee*AChE inhibition suggested that electron-withdraw substituents could promote the inhibitory activities against *ee*AChE, and the presence of OCH_3 also retained the AChE inhibition. For instance, compound **4h** with NO_2 substituent (IC_{50} = 0.055 μM, for *ee*AChE) was more effective than compound **4d** (IC_{50} = 0.18 μM, for *ee*AChE). However, *eq*BuChE inhibition was slightly lower by the substituents on FA. Moreover, inhibitory activities against ChEs were also influenced by the different substituents on the benzylamino group. Firstly, to better explain the importance of carbamate pharmacophore in ChEs inhibition, compounds **4m-o** without carbamate were further synthesized. Compared with compounds **4a-h**, the compounds **4m-o (**without carbamate pharmacophore) reduced ChEs inhibitory activity. For example, compound **4f** (IC_{50} = 0.086 μM, toward *ee*AChE) was more effective than compound **4n** (IC_{50} = 31.67 μM, for *ee*AChE), which suggested the carbamate was certainly essential to ChEs inhibition. Lastly, the substituted groups (R_2) on the carbamate also influenced the ChEs inhibition. Compounds **4d** and **4f-h** possessing N-methyl groups showed higher *ee*AChE inhibition than compounds **4i-k** with N-ethyl groups, which implied that small substituents were in favor of *ee*AChE inhibition. However, the terminal amino groups of the carbamate moiety little affected the *eq*BuChE inhibitory activities, which could

be attributed to the conformational variation between these two different enzymes in the preceding studies [38].

Furthermore, compounds **4f-h** were selected for evaluation on *h*ChE. As listed in Table 2, all tested compounds showed a high selectivity for *h*AChE over *h*BuChE and presented IC_{50} values in the nanomolar range for *h*AChE, which were slightly more potent inhibitors for *h*AChE than for *ee*AChE. The SARs for *h*AChE were similar to those drawn for *ee*AChE inhibition (Table 1). Compound **4h** (IC_{50} = 13.7 nM for *h*AChE) displayed the highest inhibition, which was 2.2-fold higher than that of standard donepezil (IC_{50} = 30.2 nM). However, the *h*BuChE inhibition of the tested derivatives was relatively low (in the micromolar range), and compound **4g** (IC_{50} = 0.0.59 μM) exhibited the most potent inhibitory activity for *h*BuChE.

2.3 Effect on self-induced Aβ (1-42) aggregation

After all FA derivates were evaluated for ChEs inhibition, they were tested for their A*β* (1-42) aggregation inhibition using a thioflavin T-based fluorometric method [39]. In the test, FA and Curcumin were used as positive references. As the results shown (Table. 3), compounds **4a-o** exhibited middle to good efficiency (37.8-51.4%, 20 μM) compared with curcumin (58.4%, 20 μM) and FA (36.7%, 20 μM). It was notable that compound **4j** (51.4%, 20 μM) showed the best inhibition. From the inhibitive activities of compounds **4a-e**, it indicated that the linker length played a minor role in the A*β* (1-42) aggregation inhibition.

Moreover, compared with compounds **4m-n**, compounds **4f-l** introducing the carbamate pharmacophore slightly increased A*β* (1-42) inhibitory activity. And compounds **4f-g** and **4j-k** with the methoxy or hydroxyl substituents on the cinnamic acid were excellent A*β* aggregation inhibitors, ranging from 49.2 to 51.4% at 20 μM. For instance, compound **4g** (49.2% at 20 μM) was more effective than that of compound **4d** (40.9% at 20 μM). This proved that the methoxy and hydroxyl groups might favor A*β* aggregation inhibition.

2.4 Antioxidant activity of compounds

During the treatment of AD, the protection of nerve cells from oxidative stress is necessary. With this understanding, the antioxidant abilities of the FA derivatives were estimated by the ABTS [2,2′-azino-bis(3-ethylbenzothiazoline-6-sulfonic acid)] radical scavenging analysis, and trolox (a vitamin E analog) was applied as the reference [40]. The scavenge radicals abilities of FA derivatives were valued by the trolox equivalent (at 25 μM). The results (in Table 3) indicated the ordinary anti-oxidative abilities of FA derivatives ranging from 0.38-1.26 trolox equivalents. Among these FA derivatives, compound **4g** exhibited the most efficient antioxidant ability with ABTS standards of 1.26 trolox equivalents, which was similar with FA (1.12 trolox equivalents). This finding could be attributed to the hydroxy group of cinnamic acid part. Based on its powerful inhibition of ChEs and Aβ (1-42) aggregation, compound **4g** with good antioxidant ability was selected as the most talented compound to continue the further study.

2.5 Kinetic study for ChEs inhibition.

Based on the excellent multi-target activities of compound **4g**, such as the potent ChE inhibition (IC_{50}, 19.7 nM for *h*AChE and 0.66 μM for *h*BuChE), the good Aβ aggregation inhibition (49.2% at 20 μM), and the good antioxidant (1.26 trolox equivalents), we further investigated the dual-site mechanism of compound **4g**. The Lineweaver-Burk graphics were applied to measure the type of AChE inhibition of compound **4g** [41]. The results in Fig. 2A suggested that the slopes and intercepts were both increased with the accumulating concentration of compound **4g**. The pattern implied compound **4g** was a mixed-type inhibitor for AChE and could simultaneously react to the catalytic active site (CAS) and the peripheral anionic site (PAS) of AChE. By comparison, a diverse plot for BuChE was picked up, exhibiting increasing slopes and constant intercepts in diverse inhibitor concentrations (Fig. 2B). The results implied that these compounds competed for the same binding site as the substrate acetylcholine.

2.6 Molecular modeling research of ChEs inhibition.

A molecular docking between compound **4g** and ChEs was studied by the software package MOE 2008.10.43. The X-ray crystal structure of the *h*AChE complex with donepezil (PDB code 1EVE) was used to contribute the origin model of *h*AChE. As the results in Fig. 3A and 3C, the benzylamino part of compound **4g** was bound to the CAS of *h*AChE, through aromatic π-π stacking interactions with the phenyl ring from Trp 84 with the ring-to-ring distance of 2.66 Å. What's more, the charged nitrogen was also bound to the CAS via a cation–*π* interaction with Tyr 334 and Phe 330. Moreover, the FA fragment inhabited the PAS formed by Asp 285, Phe 284 and Leu 282, and a hydrogen bond formed between the hydroxy of the ligands and Ser 286 with the distance of 3.19 Å. These results above indicated that compound **4g** could concurrently bind to AChE via PAS and CAS.

To explain the bind model of compound **4g**/*h*BuChE, the crystal structure of *h*BuChe (PDB code 1P0I) was applied. As the result in Fig. 4B and 4D, the benzylamino part of compound **4g** stacked up against the Tyr 332 by a cation–*π* interaction with the distance of 3.04 Å. Meanwhile, the phenyl ring of FA interactions with His 438 by a cation–*π* interaction.

2.7 Docking studies of inhibition of Aβ (1-42)

According to the good inhibition of self-induced A*β* (1-42) aggregation, we further explored the interaction mode between compound **4g** and A*β* (1-42). Molecular docking research was performed using the X-ray crystal structure of the protein A*β* structure (PDB 1IYT) [41]. As suggested in Fig. 4, the benzene ring of FA combined with the His 6 by a *π*-*π* stacking interaction with the distance of 2.63 Å. This result implied that the *π*-*π* stacking interaction of the **4g**/A*β* (1-42) complex was important in the inhibition of A*β* (1-42).

2.8 Cell viability and neuroprotection activity assay

Based on the good antioxidant activity of FA derivatives, the neuroprotection activity

of the most efficient compound **4g** was investigated *in vitro*. Firstly, neuroblastoma cell line PC12 was exposed to compound **4g** ranging from 6-100 μM. As the result in Fig. 5, compound **4g** showed low cytotoxic activity at 6-100 μM by methyl thiazolyl tetrazolium (MTT) assay.

According to the results above, the neuroprotective effects of the novel FA derivatives against H_2O_2-induced oxidative stress and Aβ (1-42)-induced cell damage were furthered explored [42]. Hydrogen peroxide (H_2O_2) was applied to cause oxidative damage in PC12 cells. As the results shown in Fig. 6A, compound **4g** obviously increased the cell viability on H_2O_2-induced oxidative cell damage in PC12 cells. Compound **4g** exhibited a powerful protection at the dose of 5 μM or 10 μM, especially with high cell viability of 70.17 % at 10 μM. These results indicated that the FA derivatives had excellent antioxidant abilities in the AD treatment. And we have also evaluated the neuroprotective effects of compound **4g** against Aβ-induced neuronal death of PC12 cells, the data were recorded after the cells were exposed to increasing concentrations of compound **4g** (6-50 μM) for 24h. As can be seen in Fig. 6B, treatment of cells with Aβ (1–42) (25 μM) markedly reduced cell viability to 47.9% compared with the untreated cells (control). Compound **4g** exhibited neuroprotective effects at concentrations ranging from 6 to 50 μM (6 μM: 48.8 ± 3.2%; 12.5 μM: 55.4 ± 2.1%; 25 μM: 58.9 ± 2.9%; 50 μM: 64.7 ± 3.8%). These observations further showed that novel cinnamic acid derivatives can inhibit Aβ (1-42) self-aggregation for the treatment of AD.

2.9 ADMET prediction and in vitro blood–brain barrier permeation assay.

Not only the good pharmacological activity is necessary, but also the pharmacokinetic property is a key to develop a drug. Recently, vital improvement in combinatorial chemistry does favor to the assessment of novel compounds' absorption, distribution, metabolism and excretion (ADME) [43]. Thus, ADME properties of the new FA derivatives **4a-o** were calculated using online Molinspiration property program [44]. The rule requests that an orally active drug can't be against one violation.

The theoretical calculations of ADME parameters (molecular weight, topological polar surface area (tPSA), log P, number of hydrogen acceptors, number of hydrogen donors, number of rotatable bonds and volume) were shown in Table 4, including the violations of Lipinski's rule. All the compounds **4a-o** conformed to Lipinski's rule which was none violation and might penetrate into the brain. This result suggests that target compounds may have good pharmacokinetics properties.

To develop central nervous system (CNS) drugs, the first requirement is crossing the BBB. Therefore, to determine the BBB penetration of our present compounds, a parallel artificial membrane permeation assay (PAMPA) was used [45]. After comparing the experimental permeability with the reported values of 9 commercial drugs (Table 5), a plot of experiment data versus the bibliographic values gave a good linear correlation: P_e (exp.) = 1.0436P_e (bibl.) – 0.2325 (R^2 = 0.9531). Based on this equation and considering the limit established by Di *et al*. for BBB permeation, we determined that compounds with permeabilities above 3.94*10^{-6} cm s^{-1} could across the BBB:

(a) ' CNS + ' (high BBB permeation predicted): *Pe* (10^{-6} cm s^{-1}) > 3.94.

(b) ' CNS - ' (low BBB permeation predicted): *Pe* (10^{-6} cm s^{-1}) < 1.85.

(c) ' CNS +/- ' (BBB permeation uncertain): *Pe* (10^{-6} cm s^{-1}) from 3.94 to 1.85.

Finally, compounds **4f** and **4g** with potent inhibitory activities against ChEs and Aβ (1-42) aggregation were selected to evaluate the BBB penetration. It can be seen that compounds **4f** and **4g** showed the Pe value higher than 3.94*10^{-6} cm s^{-1} (Table 6), which suggested that they were able to cross the BBB and might reach the biological targets located in the CNS.

3. Conclusions

Finally, we designed and synthesized a series of novel FA derivatives **4a-4o**. These compounds were proved as anti-AD agents with multi-target activities, according to their good antioxidant activity and excellent inhibitory activities on ChEs and Aβ (1-42) aggregation. Based on the screened results, compound **4g** displayed a dual inhibitory potency on both AChE and BuChE. Furthermore, the kinetic characterization

indicated that compound **4g** performed as a duel-site inhibitor binding to the CAS and the PAS of AChE, which matched to the results of the molecular modelling. Compound **4g** also exhibited the ability of inhibition of self-induced Aβ (1-42) aggregation and good antioxidant activity (1.26 trolox equivalents). What's more, the compound **4g** had the neuroprotection activity against H_2O_2-induced oxidative stress and Aβ (1-42)-induced cell damage and showed high brain penetration capacity. Generally, compound **4g** was a multifunctional cholinesterase inhibitor and applied as a potential clinical theraphy medicine for AD.

4. Experimental section

4.1 Chemistry

All chemicals (reagent grade) applied during the whole experiment were obtained from Sino pharm Chemical Reagent Co., Ltd. (China). XT-4 micromelting point instrument and uncorrected was used to measure the melting point of novel compounds. ^{1}H NMR and ^{13}C NMR spectra were tested on a BRUKER AVANCE III spectrometer at 25°C and TMS was used as the reference. Chemical shifts were recorded in ppm (δ) using the residual solvent line as internal standard. Mass spectra were recorded on a MS Agilent 1100 Series LC/MSD Trap mass spectrometer (ESI-MS).

4.2 General procedure for the synthesis of compounds

4.2.1. General procedure for the synthesis of intermediates **2a**–**h**

Compounds **2a**–**h** were easily prepared as described in the literature with some modification [33]. Compound **1** (1 mmol) and corresponding dibromo-alkanes (2 mmol) were added to acetone (30 ml), and the mixture was refluxed in the presence of Et_3N for 5 h. When the reaction was completed as shown by TLC, the mixture was cooled to room temperature and evaporated under vacuum. The crude product was purified using a silica gel column to get compound **2** with high yields.

4.2.1.1 2-Bromoethyl cinnamate (**2a**)

Cinnamic acid was reacted with 1,2-dibromoethane following the general procedure to give compound **2a** as a yellow oil (75% yield); ESI/MS m/z: 255.1 $[M+H]^+$.

4.2.1.2 3-Bromopropyl cinnamate (**2b**)

Cinnamic acid was reacted with 1,3-dibromopropane following the general procedure to give compound **2b** as a yellow oil (82% yield); ESI/MS m/z: 269.2 $[M+H]^+$.

4.2.1.3 4-Bromobutyl cinnamate (**2c**)

Cinnamic acid was reacted with 1,4-dibromobutane following the general procedure to give compound **2c** as a yellow oil (79% yield); ESI/MS m/z: 283.0 $[M+H]^+$.

4.2.1.4 5-Bromopentyl cinnamate (**2d**)

Cinnamic acid was reacted with 1,5-dibromopentane following the general procedure to give compound **2d** as a yellow oil (80% yield); ESI/MS m/z: 297.1 $[M+H]^+$.

4.2.1.5 8-Bromooctyl cinnamate (**2e**)

Cinnamic acid was reacted with 1,8-dibromooctane following the general procedure to give compound **2e** as a yellow oil (70% yield); ESI/MS m/z: 339.1 $[M+H]^+$.

4.2.1.6 (*E*)-5-bromopentyl 3-(3,4-dimethoxyphenyl)acrylate (**2f**)

(*E*)-3-(3,4-dimethoxyphenyl)acrylic acid was reacted with 1,5-dibromopentane following the general procedure to give compound **2f** as a yellow oil (82% yield); ESI/MS m/z: 357.1 $[M+H]^+$.

4.2.1.7 (*E*)-5-bromopentyl 3-(4-hydroxy-3-methoxyphenyl)acrylate (**2g**)

(*E*)-3-(4-hydroxy-3-methoxyphenyl)acrylic acid was reacted with 1,5-dibromopentane following the general procedure to give compound **2g** as a yellow oil (70% yield); ESI/MS m/z: 343.0 $[M+H]^+$.

4.2.1.8 (*E*)-5-bromopentyl 3-(4-nitrophenyl)acrylate (**2h**)

(*E*)-3-(4-nitrophenyl)acrylic acid was reacted with 1,5-dibromopentane following the general procedure to give compound **2h** as a yellow oil (82% yield); ESI/MS m/z: 342.1 $[M+H]^+$.

4.2.2. General procedure for the synthesis of intermediates **4a**–**o**

Compound **2** (3 mmol) and K_2CO_3 (12 mmol) in CH_3CN (15 ml) was stirred, then the solution of Compound **3** (3.3 mmol) in CH_3CN (5 ml) was added to the reaction mixture. After the mixture was refluxed for 12-18 h, the reaction mixture was evaporated under vacuum and extracted with ethyl acetate. The combined organic layer was washed with water, dried over anhydrous sodium sulfate, filtered, and concentrated under reduced pressure. The residue was purified by silica gel chromatography using CH_2Cl_2/MeOH as eluent to obtain target compounds **4**.

4.2.2.1 2-((3-((dimethylcarbamoyl)oxy)benzyl)(methyl)amino)ethyl cinnamate (**4a**)

Compound **2a** was reacted with compound **3a** following the general procedure to give compound **4a** as a yellow oil (45% yield); ^{1}H NMR (400 MHz, $CDCl_3$) δ 7.68 (d, *J* = 16.0 Hz, 1H), 7.49 (dd, *J* = 6.6, 2.9 Hz, 2H), 7.39 (dd, *J* = 6.4, 3.7 Hz, 3H), 7.33 – 7.29 (m, 1H), 7.17 (d, *J* = 7.6 Hz, 1H), 7.12 (s, 1H), 7.01 (dd, *J* = 8.0, 1.6 Hz, 1H), 6.43 (d, *J* = 16.0 Hz, 1H), 4.28 (t, *J* = 6.5 Hz, 2H), 3.52 (s, 2H), 3.11 (s, 3H), 3.03 (s, 3H), 2.52 (t, *J* = 7.1 Hz, 2H), 2.21 (s, 3H); ^{13}C NMR (100 MHz, $CDCl_3$) δ 167.03, 154.97, 151.58, 144.60, 140.58, 134.50, 130.21, 128.95, 128.88, 128.07, 125.70, 122.18, 120.35, 118.28, 62.96, 61.99, 53.75, 42.17, 36.57, 36.48; ESI-MS: 385.2 $[M+H]^+$.

4.2.2.2 3-((3-((dimethylcarbamoyl)oxy)benzyl)(methyl)amino)propyl cinnamate (**4b**)

Compound **2b** was reacted with compound **3a** following the general procedure to give compound **4b** as a yellow oil (52% yield); ^{1}H NMR (400 MHz, $CDCl_3$) δ 7.67 (d, *J* = 16.0 Hz, 1H), 7.54 (dd, *J* = 6.6, 2.9 Hz, 2H), 7.40 (dd, *J* = 6.4, 3.7 Hz, 3H), 7.31 – 7.28 (m, 1H), 7.17 (d, *J* = 7.6 Hz, 1H), 7.13 (s, 1H), 7.01 (dd, *J* = 8.0, 1.6 Hz, 1H), 6.43 (d, *J* = 16.0 Hz, 1H), 4.30 (t, *J* = 6.5 Hz, 2H), 3.54 (s, 2H), 3.10 (s, 3H), 3.02 (s, 3H), 2.54 (t, *J* = 7.1 Hz, 2H), 2.25 (s, 3H), 1.98 – 1.90 (m, 2H); ^{13}C NMR (100 MHz, $CDCl_3$) δ 167.02, 154.97, 151.58, 144.59, 140.55, 134.50, 130.21, 128.96, 128.86, 128.08, 125.69, 122.19, 120.37, 118.26, 62.86, 61.98, 53.78, 42.07, 36.68, 36.43, 26.66. ESI-MS: 397.2 $[M+H]^+$.

4.2.2.3 4-((3-((dimethylcarbamoyl)oxy)benzyl)(methyl)amino)butyl cinnamate (**4c**)

Compound **2c** was reacted with compound **3a** following the general procedure to give compound **4c** as a yellow oil (50% yield); ^{1}H NMR (400 MHz, $CDCl_3$) δ 7.70 (d,

J = 16.0 Hz, 1H), 7.54 (dd, *J* = 6.6, 2.8 Hz, 2H), 7.42 – 7.38 (m, 3H), 7.34 – 7.30 (m, 1H), 7.16 (d, *J* = 7.6 Hz, 1H), 7.11 (s, 1H), 7.02 (dd, *J* = 8.0, 1.5 Hz, 1H), 6.46 (d, *J* = 16.0 Hz, 1H), 4.24 (t, *J* = 6.5 Hz, 2H), 3.52 (s, 2H), 3.11 (s, 3H), 3.02 (s, 3H), 2.49 – 2.42 (m, 2H), 2.22 (s, 3H), 1.76 (dd, *J* = 14.7, 6.4 Hz, 2H), 1.66 (dd, *J* = 14.8, 8.0 Hz, 2H); ^{13}C NMR (100 MHz, $CDCl_3$) δ 167.05, 154.97, 151.58, 144.62, 140.66, 134.49, 130.21, 128.93, 128.87, 128.06, 125.71, 122.20, 120.33, 118.28, 64.53, 61.92, 56.99, 42.07, 36.67, 36.44, 26.62, 23.86; ESI-MS: 409.3 $[M+H]^+$.

4.2.2.4 5-((3-((dimethylcarbamoyl)oxy)benzyl)(methyl)amino)pentyl cinnamate (**4d**)

Compound **2d** was reacted with compound **3a** following the general procedure to give compound **4d** as a yellow oil (45% yield);^{1}H NMR (400 MHz, $CDCl_3$) δ 7.69 (d, *J* = 16.0 Hz, 1H), 7.55 – 7.52 (m, 2H), 7.41 – 7.37 (m, 3H), 7.30 – 7.27 (m, 1H), 7.17 (s, 1H), 7.13 – 7.11 (m, 1H), 7.01 (d, *J* = 8.0 Hz, 1H), 6.45 (d, *J* = 16.0 Hz, 1H), 4.21 (t, *J* = 6.6 Hz, 2H), 3.52 (s, 2H), 3.10 (s, 3H), 3.09 (s, 3H), 2.46 – 2.40 (m, 2H), 2.22 (s, 3H), 1.77 – 1.68 (m, 2H), 1.60 (dt, *J* = 15.0, 7.4 Hz, 2H), 1.49 – 1.39 (m, 2H); ^{13}C NMR (100 MHz, $CDCl_3$) δ 167.02, 154.97, 151.58, 144.59, 140.55, 134.50, 130.21, 128.96, 128.86, 128.08, 125.69, 122.19, 120.37, 118.26, 62.86, 61.98, 53.78, 42.07, 36.68, 36.43, 26.66; ESI-MS: 421.3 $[M+H]^+$.

4.2.2.5 8-((3-((dimethylcarbamoyl)oxy)benzyl)(methyl)amino)octyl cinnamate (**4e**)

Compound **2e** was reacted with compound **3a** following the general procedure to give compound **4e** as a yellow oil (42% yield);^{1}H NMR (400 MHz, $CDCl_3$) δ 7.70 (d, *J* = 16.0 Hz, 1H), 7.54 (dd, *J* = 6.6, 2.8 Hz, 2H), 7.41 – 7.36 (m, 3H), 7.29 (t, *J* = 3.9 Hz, 1H), 7.16 (d, *J* = 7.7 Hz, 1H), 7.11 (s, 1H), 7.02 (d, *J* = 8.0 Hz, 1H), 6.46 (d, *J* = 16.0 Hz, 1H), 4.21 (t, *J* = 6.7 Hz, 2H), 3.52 (s, 2H), 3.11 (d, *J* = 4.8 Hz, 3H), 3.01 (s, 3H), 2.46 – 2.33 (m, 2H), 2.21 (s, 3H), 1.75 – 1.67 (m, 2H), 1.54 (s, 2H), 1.41 – 1.31 (m, 8H); ^{13}C NMR (100 MHz, $CDCl_3$) δ 167.02, 154.97, 151.58, 144.59, 140.55, 134.50, 130.21, 128.96, 128.86, 128.08, 125.69, 122.19, 120.37, 118.26, 62.86, 61.98, 53.78, 42.07, 36.68, 36.43, 26.66. ESI-MS: 457.2 $[M+H]^+$.

4.2.2.6 (*E*)-5-((3-((dimethylcarbamoyl)oxy)benzyl)(methyl)amino)pentyl-3-(3,4-dimethoxyphenyl)acrylate (**4f**)

Compound **2f** was reacted with compound **3a** following the general procedure to give compound **4f** as a yellow oil (52% yield); ^{1}H NMR (400 MHz, $CDCl_3$) δ 7.64 (d, *J* = 15.9 Hz, 1H), 7.33–7.28 (m, 1H), 7.19 – 7.10 (m, 3H), 7.08 (d, *J* = 1.9 Hz, 1H), 7.02 (dd, *J* = 8.0, 1.6 Hz, 1H), 6.88 (d, *J* = 8.3 Hz, 1H), 6.34 (d, *J* = 15.9 Hz, 1H), 4.21 (t, *J* = 6.6 Hz, 2H), 3.93 (d, *J* = 4.6 Hz, 6H), 3.52 (s, 2H), 3.11 (s, 3H), 3.02 (s, 3H), 2.46–2.39 (m, 2H), 2.22 (s, 3H), 1.79–1.68 (m, 2H), 1.60 (dt, *J* = 14.9, 7.4 Hz, 2H), 1.51–1.41 (m, 2H); ^{13}C NMR (100 MHz, $CDCl_3$) δ 167.35, 154.99, 151.54, 151.08, 149.20, 144.53, 140.77, 128.93, 127.46, 125.74, 122.62, 122.22, 120.30, 115.96, 111.03, 109.59, 64.53, 62.00, 57.37, 55.98, 55.89, 42.22, 36.69, 36.44, 28.71, 27.06, 23.86; ESI-MS: 485.2 $[M+H]^+$.

4.2.2.7 (*E*)-5-((3-((dimethylcarbamoyl)oxy)benzyl)(methyl)amino)pentyl-3-(4-hydroxy-3-methoxyphenyl)acrylate (**4g**)

Compound **2g** was reacted with compound **3a** following the general procedure to give compound **4g** as a yellow oil (43% yield); ^{1}H NMR (400 MHz, $CDCl_3$) δ 7.73 (d, *J* = 15.9 Hz, 1H), 7.39 – 7.30 (m, 1H), 7.25 – 7.15 (m, 3H), 7.10 (d, *J* = 1.9 Hz, 1H), 7.05 (dd, *J* = 8.0, 1.6 Hz, 1H), 6.90 (d, *J* = 8.3 Hz, 1H), 6.35 (d, *J* = 15.9 Hz, 1H), 4.22 (t, *J* = 6.6 Hz, 2H), 3.90 (d, *J* = 4.6 Hz, 6H), 3.52 (s, 2H), 3.12 (s, 3H), 2.46 – 2.39 (m, 2H), 2.24 (s, 3H), 1.79 – 1.65 (m, 2H), 1.63 (dt, *J* = 14.9, 7.4 Hz, 2H), 1.51 – 1.45 (m, 2H); ^{13}C NMR (100 MHz, $CDCl_3$) δ 166.49, 154.75, 152.08, 151.35, 149.26, 144.55, 140.71, 128.72, 127.43, 124.94, 122.53, 122.13, 120.51, 116.32, 111.72, 108.43, 64.65, 62.06, 57.39, 55.38, 41.53, 36.50, 36.16, 28.70, 27.08, 23.46; ESI-MS: 471.3 $[M+H]^+$.

4.2.2.8 (*E*)-5-((3-((dimethylcarbamoyl)oxy)benzyl)(methyl)amino)pentyl-3-(4-nitrophenyl)acrylate (**4h**)

Compound **2h** was reacted with compound **3a** following the general procedure to give compound **4h** as a yellow oil (58% yield); ^{1}H NMR (400 MHz, $CDCl_3$) δ 8.27 (d, *J* = 8.6 Hz, 2H), 7.71 (t, *J* = 11.9 Hz, 3H), 7.33 (d, *J* = 7.8 Hz, 1H), 7.19 (d, *J* = 7.7 Hz, 1H), 7.13 (s, 1H), 7.05 (d, *J* = 7.5 Hz, 1H), 6.58 (d, *J* = 16.1 Hz, 1H), 4.25 (t, *J* = 6.6 Hz, 2H), 3.60 (s, 2H), 3.11 (s, 3H), 3.02 (s, 3H), 2.54 – 2.45 (m, 2H), 2.26 (d, *J* = 10.4 Hz, 3H), 1.74 (dd, *J* = 14.5, 7.0 Hz, 2H), 1.69 – 1.59 (m, 2H), 1.47 (d, *J* = 7.1 Hz, 2H);

^{13}C NMR (100 MHz, $CDCl_3$) δ 166.12, 154.96, 151.55, 148.46, 141.62, 140.73, 140.59, 128.93, 128.65, 125.69, 124.15, 122.59, 122.20, 120.31, 65.09, 61.97, 57.27, 42.23, 36.68, 36.44, 28.57, 27.01, 23.78; ESI-MS: 470.2.

4.2.2.9 5-((3-((ethyl(methyl)carbamoyl)oxy)benzyl)(methyl)amino)pentyl cinnamate (**4i**)

Compound **2d** was reacted with compound **3b** following the general procedure to give compound **4i** as a yellow oil (50% yield); ^{1}H NMR (400 MHz, $CDCl_3$) δ 7.70 (d, *J* = 16.0 Hz, 1H), 7.55 (dd, *J* = 6.4, 2.8 Hz, 2H), 7.43 – 7.37 (m, 3H), 7.32 (d, *J* = 7.7 Hz, 1H), 7.17 (dd, *J* = 21.2, 13.1 Hz, 2H), 7.05 (s, 1H), 6.46 (dd, *J* = 16.0, 3.3 Hz, 1H), 4.23 (dd, *J* = 11.6, 5.0 Hz, 2H), 3.56 (s, 2H), 3.53 – 3.37 (m, 4H), 3.08 (s, 2H), 2.99 (d, *J* = 8.6 Hz, 2H), 2.51 – 2.42 (m, 2H), 2.25 (s, 3H), 1.73 (dd, *J* = 14.7, 7.0 Hz, 2H), 1.67 – 1.58 (m, 2H), 1.46 (dd, *J* = 15.2, 8.1 Hz, 2H), 1.22 (d, *J* = 13.8 Hz, 3H); ^{13}C NMR (100 MHz, $CDCl_3$) δ 167.11, 151.57, 144.64, 134.47, 130.23, 129.37, 129.00, 128.88, 128.08, 125.83, 123.54, 122.37, 120.89, 120.52, 120.24, 118.26, 64.84, 64.60, 61.81, 57.19, 50.85, 44.07, 42.03, 34.24, 33.80, 29.71, 28.65, 26.83, 23.83, 13.23, 12.47; ESI-MS: 439.3.

4.2.2.10 (*E*)-5-((3-((ethyl(methyl)carbamoyl)oxy)benzyl)(methyl)amino)pentyl-3-(3,4-dimethoxyphenyl)acrylate (**4j**)

Compound **2f** was reacted with compound **3b** following the general procedure to give compound **4j** as a yellow oil (54% yield); ^{1}H NMR (400 MHz, $CDCl_3$) δ 7.62 (d, *J* = 15.9 Hz, 1H), 7.28 (dd, *J* = 11.0, 4.6 Hz, 1H), 7.16 – 7.02 (m, 4H), 6.99 (d, *J* = 7.8 Hz, 1H), 6.85 (dd, *J* = 8.3, 2.8 Hz, 1H), 6.31 (d, *J* = 15.9 Hz, 1H), 4.19 (t, *J* = 6.6 Hz, 2H), 3.89 (d, *J* = 3.3 Hz, 7H), 3.51 – 3.34 (m, 4H), 3.01 (d, *J* = 30.9 Hz, 3H), 2.19 (s, 3H), 1.75 – 1.66 (m, 2H), 1.57 (dt, *J* = 14.9, 7.4 Hz, 2H), 1.44 (dd, *J* = 15.2, 8.2 Hz, 2H), 1.26 – 1.13 (m, 4H); ^{13}C NMR (100 MHz, $CDCl_3$) δ 167.32, 151.55, 151.06, 149.19, 144.52, 128.92, 127.44, 125.69, 122.61, 122.23, 120.34, 115.94, 111.02, 109.58, 64.50, 61.95, 57.32, 55.96, 55.88, 44.05, 42.19, 28.71, 27.01, 23.86; ESI-MS: 499.3 $[M+H]^+$.

4.2.2.11 (*E*)-5-((3-((ethyl(methyl)carbamoyl)oxy)benzyl)(methyl)amino)pentyl-3-

(4-hydroxy-3-methoxyphenyl)acrylate (**4k**)

Compound **2g** was reacted with compound **3b** following the general procedure to give compound **4k** as a yellow oil (44% yield); ^{1}H NMR (400 MHz, $CDCl_3$) δ 7.63 (dd, *J* = 15.9, 3.2 Hz, 1H), 7.38 – 7.30 (m, 1H), 7.16 (d, *J* = 7.0 Hz, 1H), 7.07 (m, 4H), 6.90 (dd, *J* = 20.9, 8.2 Hz, 1H), 6.31 (dt, *J* = 15.9, 3.4 Hz, 1H), 4.21 (t, *J* = 6.6 Hz, 2H), 4.13 – 3.78 (m, 5H), 3.62 – 3.35 (m, 5H), 3.08 (d, *J* = 6.2 Hz, 2H), 3.00 (s, 3H), 2.54 – 2.34 (m, 2H), 2.23 (s, 3H), 1.78 – 1.67 (m, 2H), 1.62 (dd, *J* = 15.2, 6.9 Hz, 2H), 1.46 (dd, *J* = 15.2, 8.2 Hz, 2H), 1.25 – 1.16 (m, 3H). ^{13}C NMR (100 MHz, $CDCl_3$) δ 167.39, 151.56, 147.99, 146.83, 144.72, 128.98, 125.81, 123.07, 122.57, 122.36, 120.48, 115.59, 114.75, 112.41, 110.11, 109.35, 68.72, 64.46, 61.84, 57.25, 55.94, 50.86, 44.07, 42.07, 29.71, 28.70, 26.87, 23.86; ESI-MS: 485.3 $[M+H]^+$.

4.2.2.12 (*E*)-5-((3-((ethyl(methyl)carbamoyl)oxy)benzyl)(methyl)amino)pentyl 3-(4-nitrophenyl)acrylate (**4l**)

Compound **2h** was reacted with compound **3b** following the general procedure to give compound **4l** as a yellow oil (40% yield); ^{1}H NMR (400 MHz,) δ 8.24 (d, *J* = 7.9 Hz), 7.68 (dd, *J* = 16.9, 12.3 Hz), 7.28 (d, *J* = 8.0 Hz), 7.11 (dd, *J* = 30.4, 6.4 Hz), 7.00 (s), 6.56 (d, *J* = 16.0 Hz), 4.22 (t, *J* = 6.5 Hz), 3.48 (s), 3.05 (s), 2.98 (s), 2.39 (t, *J* = 7.1 Hz), 2.19 (s), 1.71 (dd, *J* = 14.4, 6.9 Hz), 1.57 (dt, *J* = 14.9, 7.4 Hz), 1.48 – 1.38 (m), 1.28 – 1.21 (m); ^{13}C NMR (100 MHz, $CDCl_3$) δ 166.15, 151.55, 148.47, 141.65, 140.60, 128.96, 128.67, 125.73, 124.18, 122.59, 122.27, 120.37, 65.11, 61.99, 57.29, 44.07, 42.24, 34.25, 33.82, 28.58, 27.00, 23.80; ESI-MS: 484.3 $[M+H]^+$.

4.2.2.13 5-(benzyl(methyl)amino)pentyl cinnamate (**4m**)

Compound **2d** was reacted with compound **3c** following the general procedure to give compound **4k** as a yellow oil (65% yield); ^{1}H NMR (400 MHz, $CDCl_3$) δ 7.68 (d, *J* = 16.0 Hz, 1H), 7.53 (dd, *J* = 6.5, 2.9 Hz, 2H), 7.43 – 7.36 (m, 3H), 7.33 (d, *J* = 6.2 Hz, 3H), 7.26 (s, 2H), 6.44 (d, *J* = 16.0 Hz, 1H), 4.20 (t, *J* = 6.6 Hz, 2H), 3.55 (s, 2H), 2.55 – 2.31 (m, 2H), 2.24 (s, 3H), 1.76 – 1.66 (m, 2H), 1.61 (dd, *J* = 14.9, 7.6 Hz, 2H), 1.49 – 1.39 (m, 2H); ^{13}C NMR (100 MHz, $CDCl_3$) δ 167.09, 144.66, 134.47, 130.25,

129.27, 128.89, 128.34, 128.08, 127.25, 118.24, 64.54, 57.03, 41.96, 28.63, 26.71, 23.81; ESI-MS: 338.2 $[M+H]^+$.

4.2.2.14 (*E*)-5-(benzyl(methyl)amino)pentyl 3-(3,4-dimethoxyphenyl)acrylate (**4n**)

Compound **2f** was reacted with compound **3c** following the general procedure to give compound **4k** as a yellow oil (68% yield); ^{1}H NMR (400 MHz, $CDCl_3$) δ 7.63 (d, *J* = 15.9 Hz, 1H), 7.36 – 7.27 (m, 4H), 7.26 – 7.22 (m, 1H), 7.10 (dd, *J* = 8.3, 1.8 Hz, 1H), 7.06 (d, *J* = 1.8 Hz, 1H), 6.87 (d, *J* = 8.3 Hz, 1H), 6.31 (d, *J* = 15.9 Hz, 1H), 4.20 (t, *J* = 6.6 Hz, 2H), 3.91 (d, *J* = 1.5 Hz, 6H), 3.51 (s, 2H), 2.46 – 2.34 (m, 2H), 2.21 (s, 3H), 1.70 (dd, *J* = 14.7, 7.0 Hz, 2H), 1.59 (dd, *J* = 15.0, 7.6 Hz, 2H), 1.48 – 1.40 (m, 2H); ^{13}C NMR (101 MHz, $CDCl_3$) δ 167.33, 151.09, 149.22, 144.55, 129.14, 128.26, 127.46, 127.05, 122.62, 115.94, 111.03, 109.58, 64.48, 62.25, 57.18, 55.99, 55.90, 42.13, 28.70, 26.94, 23.86; ESI-MS: 398.2 $[M+H]^+$.

4.2.2.15 (*E*)-5-(benzyl(methyl)amino)pentyl 3-(4-nitrophenyl)acrylate (**4o**)

Compound **2h** was reacted with compound **3c** following the general procedure to give compound **4k** as a yellow oil (69% yield); ^{1}H NMR (400 MHz, $CDCl_3$) δ 8.24 (d, *J* = 8.8 Hz, 2H), 7.68 (dd, *J* = 14.7, 12.4 Hz, 3H), 7.31 (d, *J* = 4.4 Hz, 4H), 7.23 (dd, *J* = 5.3, 3.4 Hz, 1H), 6.56 (d, *J* = 16.0 Hz, 1H), 4.23 (t, *J* = 6.6 Hz, 2H), 3.48 (s, 2H), 2.44 – 2.34 (m, 2H), 2.18 (d, *J* = 9.0 Hz, 3H), 1.76 – 1.68 (m, 2H), 1.58 (dt, *J* = 14.7, 7.2 Hz, 2H), 1.48 – 1.40 (m, 2H); ^{13}C NMR (101 MHz, $CDCl_3$) δ 166.11, 148.49, 141.64, 140.59, 139.17, 129.04, 128.64, 128.21, 126.93, 124.18, 122.59, 65.11, 62.36, 57.21, 42.26, 28.59, 27.06, 23.80; ESI-MS: 383.2 $[M+H]^+$.

4.3 Inhibition studies on ChEs *in vitro*

Acetylcholinesterase (AChE, E.C 3.1.1.7, from electric eel), Butyrylcholinesterase (BuChE, E.C 3.1.1.8, from equine serum), 5,5'-dithiobis (2-nitrobenzoic acid) (DTNB, Ellman's reagent), donepezil hydrochloride, acetylthiocholine iodide (ATCI) and *S*-butyrylthiocholine iodide (BTCI) were obtained from Sigma-Aldrich. Ellman's method was applied to evaluate the inhibition activities of target compounds **4a-o** towards AChE and BuChE [34]. The tested compounds were dissolved in DMSO to 1% and

diluted by the buffer solution (0.1 M NaCl, 50 mM Tris-HCl, 0.02 M $MgCl_2 \cdot 6H_2O$ pH= 8.0). For ChEs inhibition test, 160 μL DTNB (1.5 mM) was added to a 96-well plate, and mixed with 50 μL of AChE (0.22 U/mL prepared in 50 mM Tris-HCl, pH =8.0, 0.1% w/v bovine serum albumin, BSA) or 50 μL of BuChE (0.12 U/mL prepared in 50 mM Tris-HCl, pH=8.0, 0.1% w/v BSA). Then, the respective enzyme were treated with 10 μL various concentrations of test compounds (0.001-100 μM) at 37 °C for 6 min, followed by the addition of substrate (30 μL), *S*-butyrylthiocholine iodide (15 mM) or acetylthiocholine iodide (15 mM), and the absorbance at 405 nm was measured after 0, 1, 2, and 3 min. The concentration of FA derivatives producing 50% of enzyme activity inhibition (IC_{50}) was processed by the Graph-Pad Prism program package (Graph Pad Software), according to nonlinear regression analysis of the response-concentration (log) curve. The experiments were performed in triplicate and the results were exhibited as the mean ± SEM.

4.4 Kinetic analysis of AChE and BuChE inhibition

To investigate the inhibition mechanism of present compounds, compound **4g** was taken for kinetic analysis by Ellman's method [39]. Three concentrations of **4g** were selected for the study: 55, 110 and 220 nM of compound **4g** were chosen for the kinetic analysis of AChE inhibition and 1.25, 2.5 and 5 μM of compound **4g** were selected for the kinetic study of BuChE inhibition. Following a similar method mentioned above in enzyme inhibition assay, Lineweaver–Burk reciprocal plots were constructed by plotting 1/velocity against 1/[substrate] at varying concentrations of the substrate acetylthiocholine (0.05 – 0.5 mM). All measurements were performed in triplicate and data analysis was performed with Graph Pad Prism 4.03 software (San Diego, CA, USA).

4.5 Inhibition of Aβ (1-42) self-induced aggregation

The inhibitory activities of compounds on self-induced A*β* (1-42) aggregation were also measured by the ThT assay [37]. HFIP and ThT were purchased from TCI

(Shanghai) Development. Aβ (1-42) was obtained from Royobiotech Co., Ltd (Shanghai, China). The monomeric Aβ (1-42) samples were prepared by HFIP and diluted with a 50 mM phosphate buffer (pH 7.4) to give a 25 μM solution. The test compound was dissolved in DMSO (250 μM) for storage and needed not to be diluted prior to use. In each well, 1 μL of test compound at final concentration of 25 μM and 9 μL of Aβ (1-42) sample were added, and the obtained mixture was incubated in dark at room temperature for 46-48 h with no agitation. Then, 200 μL of 5 μM ThT in 50 mM glycine-NaOH buffer (pH 8.0) was added. Fluorescence intensity at 490 nm (emission at 446 nm) was measured through a SpectraMax M5 (Molecular Devices, Sunnyvale, CA, USA) with multi-mode plate reader. The fluorescence intensities of the mixture at 490 nm were collected and the percent inhibition caused by the presence of the inhibitor was calculated based on the following formula:

$$Percent\ inhibition = 100 - (IF_i / IF_o \times 100)$$

IF_i and IF_o were the fluorescence intensities of Aβ (1-42) incubated with inhibitor or buffer respectively.

4.6 Study of antioxidant capability in vitro

2,2'-Azino-bis-2-ethybenz-thiazoline-6-sulfonic acid (ABTS) radical catching method was applied to assess the antioxidant capability of the FA derivatives [38]. Firstly, ABTS (7 mM, in purified water) was treated with potassium persulfate (2.45 mM, in purified water) to form ATBS radical cation ($ABTS^{\cdot+}$), and the ABTS mixture was placed at room temperature in dark for 24 h before use. The stock solution of ABTS was then diluted to 100 μM in sodium phosphate buffer (50 mM, pH 7.4). Different concentrations of trolox and compounds **4a-o** (50 μL) were added to 150 μL prepared ABTS solution (100 μM), respectively. After the complete mixing of reactants, the absorbance of at 415 nm of the solution was measured in 6 min at 30 °C. Every individual experiment was performed for three times.

4.7 Molecular modeling research

Molecular Operating Environment (MOE) 2015.10 (Montreal, Canada) was applied to finish the molecular modeling calculations and docking research. AChE, BuChE and Aβ (1-42) were modeled by respectively locating them in the active site according to the published crystallographic structures (PDB code: 1EVE, code 1P0I, PDB 1IYT.) Then, we deleted all water molecules in PDB files and added hydrogen atoms to the protein. The compound **4g** was constructed by the builder interface of the MOE and energy minimized through MMFF94x force field. Subsequently, the compound **4g** was docked into the active site of the protein using the "Triangle Matcher" method, which induced poses by adjusting the ligand triplet of atoms with the triplet of alpha spheres in cavities of sealed atomic packing. The Dock scoring in MOE software was completed by ASE scoring utility and Force field was chosed as the improved method. 10 top-ranked conformations of compounds were recorded and stored. Finally, the geometry of docked complex was analized by the pose viewer utility in MOE.

4.8. Blood–brain barrier permeation study in vitro

The parallel artificial membrane permeation assay (PAMPA) was a common way to evaluate the brain penetration of molecules [43]. Before the experiments, all compounds were prepared in DMSO, and the stock solutions were diluted in PBS/EtOH (70: 30) to make secondary stock solutions (25 μg/mL). After the pretreatment, the filter membrane on the 96-well filtration plate (PVDF membrane, pore size 0.45 mm, Millipore) was coated with 4 μL of PBL (Avanti Polar Lipids) in dodecane (20 mg/mL, Sigma-Aldrich). Then, 300 μL of PBS/EtOH (70: 30) and 200μL of diluted solution containing the corresponding drugs or test compounds were added to corresponding acceptor well and donor well, respectively. Afterwards, the acceptor filter plate was carefully placed on the donor plate to make the coated membrane touch both donor solution and acceptor buffer. After incubation for 18 h at 25 °C, the concentrations of test compounds in reference, acceptor and donor wells were determined by a UV plate reader (SpectraMax Plus 384, Molecular Devices). All samples were analyzed in four wells, for five wavelengths, and by three independent runs. In every experiment,

various quality control standards of known BBB permeability were applied to approve the analysis set.

4.9. Cell culture and investigation of cell viability

The rat pheochromocytoma (PC12) cell was applied to test the toxicity effect of the FA derivatives. PC 12 cells was purchased from the Cell Bank of the Chinese Academy of Sciences (Shanghai, China) and cultured in Dulbecco's modified Eagle's medium (DMEM) supplemented with 10% bovine calf serum, 100 U/mL penicillin-streptomycin and incubated at 37 °C in a humidified incubator with 5% CO_2 in. Cells were seeded in 96-well plates at 5×10^3 cells/well and treated for 24h. Then, the cells were placed into serum-free medium and incubated with compound **4g**. The survival of cells was determined in 24 h by MTT assay and the absorbance at 570 nm was measured by a microculture plate reader. Results were expressed as the percentage of the control and repeated for three times.

The PC12 cells were selected to evaluate the protective capabilities of compounds against the neurotoxicity induced by hydrogen peroxide (H_2O_2) [40]. The PC12 cells were sub-cultured in 96-well plates at 2×10^4 cells/well, treated for 12 h and subsequently incubated in serum-free DMEM containing 250 μM H_2O_2 and different concentrations (1, 2.5, 5, 10 μM) of compound **4g**. Cell viability was tested by MTT assay after the incubation with 250 μM H_2O_2 for 24 h.

The PC12 cells were also selected to evaluate the protective capabilities of compounds against the neurotoxicity induced by Aβ (1-42). After pretreatment with different concentrations of compound **4g** (0, 6, 12.5, 25, 50 μM) for 2h, PC 12 cells were incubated with 25 μM of Aβ (1-42) for 24 h. The cell viability was evaluated using MTT assay.

Acknowledgments

This work was supported by programs of the National Natural Science Foundation of China [81872981 and 81760622]; Program of Shanghai Academic/Technology

Research Leader [18XD1403700]; National Scientific and Technological Major Special Project of China (2018ZX09201008-002); Youth Talent Sail Plan from the Shanghai Committee of Science and Technology [18YF1423600]; Projects sponsored by the development fund for Shanghai talents [2018105]; Project of the Shanghai Municipal Commission of Health and Family Planning [2017YQ072 and 201740152]; Research Fund for the Doctoral Program of Shanghai [B201703]; Undergraduate innovation project from Shanghai University of traditional Chinese Medicine [grant number 2019SHUTCM146] and Xinglin Young Talent Program.

Conflicts of Interest

The authors declare no conflict of interest.

References

1. W. Thies, L. Bleiler, Alzheimers Dement. 9 (2013) 208-245.

2. Alzheimer’s Association, Alzheimer's Disease Facts and Figures, Alzheimer’s Dementia.11 (2015) 332-384.

3. Alzheimer’s Disease International. World Alzheimer Report 2015: The Global Impact of Dementia.

4. Alzheimer’s Disease International World Alzheimer Report, The Global Impact of Dementia, 2015.

5. Y. Huang, L. Mucke, Alzheimer mechanisms and therapeutic strategies, Cell. 148 (2012) 1204-1222.

6. R. Jakob-Roetne and H. Jacobsen, Alzheimer's Disease: From Pathology to Therapeutic Approaches, Angew. Chem., Int. Ed. 48 (2009), 3030-3059.

7. S. Pfaender and A. M. Grabrucker, Characterization of biometal profiles in neurological disorders, Metallomics, 6 (2014) 960-977.

8. N. Herrmann, S.A. Chau, I. Kircanski, K.L. Lanctot, Current and emerging drug treatment options for Alzheimer's disease: a systematic review, Drugs. 71 (2011) 2031-2065

9. P. Anand, B. Singh, A review on cholinesterase inhibitors for Alzheimer's disease, Arch. Pharm. Res. 36 (2013) 375-399.

10. S. Darvesh, D.A. Hopkins, Neurobiology of butyrylcholinesterase, C. Geula, Nat. Rev. Neurosci. 2 (2003) 131-138.

11. Hardy J, Selkoe DJ, The amyloid hypothesis of Alzheimer's disease: progress and problems on the road to therapeutics, Science. 297 (2002) 353-356.

12. Paul S, Planque S, Nishiyama Y, Beneficial catalytic immunity to abeta peptide, Rejuvenat Res. 13 (2010) 179-187.

13. Ansari MA, Scheff SW. Oxidative stress in the progression of Alzheimer disease in the frontal cortex, J Neuropathol Exp Neurol, 69 (2010) 155–167.

14. Jiang CS, Fu Y, Zhang L, Gong JX, Wang ZZ, Xiao W, Zhang HY, Guo YW, Synthesis and biological evaluation of novel marine-derived indole-based 1,2,4-oxadiazoles derivatives as multifunctional neuroprotective agents, Bioorg Med Chem Lett. 25 (2015) 216-220.

15. Leon R, Garcia AG, Marco-Contelles J, Recent advances in the multitarget-directed ligands approach for the treatment of Alzheimer's disease, Med Res Rev. 33 (2013) 139-189.

16. Agis-Torres A, Solhuber M, Fernandez M, Sanchez-Montero JM, Multi-target- € directed ligands and other therapeutic strategies in the search of a real solution for Alzheimer's disease, Curr Neuropharmacol. 12 (2014) 2–36.

17. Bajda M, Guzior N, Ignasik M, Malawska B, Multi-target-directed ligands in Alzheimer's disease treatment, Curr Med Chem, 18 (2011) 4949-4975.

18. Jiang N, Ding J, Liu J, Sun X, Zhang Z, Mo Z, Li X, Yin H, Tang W, Xie SS, Novel chromanone-dithiocarbamate hybrids as multifunctional AChE inhibitors with β-amyloid anti-aggregation properties for the treatment of Alzheimer's disease, Bioorg Chem. 89 (2019) 103027-103038.

19. Jiang N, Huang Q, Liu J, Liang N, Li Q, Li Q, Xie SS, Design, synthesis and biological evaluation of new coumarin-dithiocarbamate hybrids as multifunctional agents for the treatment of Alzheimer's disease, Eur J Med Chem. 146 (2018) 287–298.

20. E Polo, N Ibarra-Arellano, L Prent-Peñaloza, A Morales-Bayuelo, J Henao, A Galdámez, M Gutiérrez. Ultrasound-assisted synthesis of novel chalcone, heterochalcone and bis-chalcone derivatives and the evaluation of their antioxidant properties and as acetylcholinesterase inhibitors, Bioorg Chem. 90 (2019) 103034-103044.

21. N Choubdar, M Golshani, L Jalili-Baleh, H Nadri, TT Küçükkilinç, B Ayazgök, A Moradi, FH Moghadam, Z Abdolahi, A Ameri, F Salehian, A Foroumadi, M Khoobi. New classes of carbazoles as potential multi-functional anti-Alzheimers agents, Bioorg Chem. 91 (2019) 103164-103173.

22. Sgarbossa A, Giacomazza D, di Carlo M, Ferulic acid: a hope for Alzheimer's disease therapy from plants, Nutrients. 7 (2015) 5764–5782.

23. W. Xu, X. Wang, Z. Wang, JJ. Wu, F. Li, J. Wang, LY. Kong, Synthesis and evaluation of donepezil–ferulic acid hybrids as multi-target-directed ligands against Alzheimer's disease, MedChemComm. 7 (2016), 990–998.

24. W. Pan, K. Hu, P. Bai, L. Yu, Q. Ma, T. Li, X. Zhang, C. Chen, K. Peng, W. Liu, Z. Sang, Design, synthesis and evaluation of novel ferulic acid-memoquin hybrids as potential multifunctional agents for the treatment of Alzheimer’s disease, Bioorg Med Chem Lett. 26 (2016), 2539–2543.

25. Z. Sang, W. Pan, K. Wang, Q. Ma, L. Yu, Y. Yang, P. Bai, C. Leng, Q. Xu, X. Li, Z. Tan, W. Liu, Design, synthesis and evaluation of novel ferulic acid-O-alkylamine derivatives as potential multifunctional agents for the treatment of Alzheimer's disease, Eur J Med Chem. 130 (2017), 379–392.

26. Digiacomo, M.; Chen, Z.; Wang, S.; Lapucci, A.; Macchia, M.; Yang, X.; Chu, J.; Han, Y.; Pi, R.; Rapposelli, S. Synthesis and pharmacological evaluation of multifunctional tacrine derivatives against several disease pathways of AD, Bioorg Med Chem Lett. 25 (2015), 807-810.

27. JS. Lan, JW. Hou, Y. Liu,Y. Ding, Y. Zhang, L. Li, T. Zhang, Design, synthesis and evaluation of novel cinnamic acid derivatives bearing N-benzyl pyridinium moiety as multifunctional cholinesterase inhibitors for Alzheimer’s disease, J Enzym Inhib

Med Chem. 32 (2017), 776–788.

28.L. Fang, M. Chen, Z. Liu, X. Fang, S. Gou, L. Chen, Ferulic acid-carbazole hybrid compounds: combination of cholinesterase inhibition, antioxidant and neuroprotection as multifunctional anti-Alzheimer agents, Bioorg Med Chem. 24 (2016) 886-893.

29. L. Piazzi, A. Rampa, A. Bisi, S. Gobbi, F. Belluti, A. Cavalli, M. Bartolini, V. Andrisano, P. Valenti, M. Recanatini, 3-(4-{[Benzyl(methyl)amino]methyl}-phenyl)-6,7-dimethoxy-2H-2-chromenone (AP2238) inhibits both acetylcholinesterase and acetylcholinesterase-Induced *β*-Amyloid aggregation: a dual function lead for Alzheimer's disease therapy, J Med Chem. 46 (2003) 2279-2282.

30. M. D. Gottwald, R. I. Rozanski, Rivastigmine, a brain-region selective acetylcholinesterase inhibitor for treating Alzheimer's disease: review and current status, Expert Opin Investig Drugs. 8 (1999), 1673-1682.

31. JS. Lan, Y. Liu, JW. Hou, J. Yang, XY. Zhang, Y. Zhao, SS. Xie, Y. Ding, T. Zhang. Design, synthesis and evaluation of resveratrol-indazole hybrids as novel monoamine oxidases inhibitors with amyloid-*β* aggregation inhibition, Bioorg Chem. 76 (2018) 130–139.

32. JS. Lan , T. Zhang, Y. Liu, J. Yang, SS. Xie, J. Liu, ZY. Miao, Y. Ding, Design, synthesis and biological activity of novel donepezil derivatives bearing N-benzyl pyridinium moiety as potent and dual binding site acetylcholinesterase inhibitors, Eur J Med Chem. 23 (2017) 184-196.

33. JS. Lan, Y. Ding, Y. Liu, P. Kang, JW. Hou, XY. Zhang, SS. Xie, Tong. Zhang, Design, synthesis and biological evaluation of novel coumarin-N-benzyl pyridinium hybrids as multi-target agents for the treatment of Alzheimer's disease, Eur J Med Chem. 139 (2017) 48-59.

34. SS. Xie, JS. Lan, X. Wang, ZM. Wang, N. Jiang, F. Li, JJ. Wu, J. Wang, LY. Kong, Design, synthesis and biological evaluation of novel donepezil-coumarin hybrids as multi-target agents for the treatment of Alzheimer's disease, Bioorg Med Chem. 27 (2016) 1528-1539.

35. H. Jiang, X. Wang, L. Huang, Z. Luo, T. Su, K. Ding, X. Li, Benzenediol-berberine

hybrids: Multifunctional agents for Alzheimer's disease, Bioorg Med Chem. 19 (2011) 7228–7235.

36. GL. Ellman, KD. Courtney, V. Andres, JR., RM. Featherstone, A new and rapid colorimetric determination of acetylcholinesterase activity, Biochem Pharmacol, 7 (1961) 88–95.

37. JS. Lan, SS. Xie, SY. Li, LF. Pan, XB. Wang, LY. Kong, Design, synthesis and evaluation of novel tacrine-(carboline) hybrids as multifunctional agents for the treatment of Alzheimer's disease, Bioorg Med Chem. 22 (2014) 6089-6104.

38. S. Rizzo, C. Riviere, L. Piazzi, A. Bisi, S. Gobbi, M. Bartolini, V. Andrisano, F. Morroni, A. Tarozzi, JP. Monti,. Benzofuran-based hybrid compounds for the inhibition of cholinesterase activity, beta amyloid aggregation, and abeta neurotoxicity, J Med Chem. 51 (2008) 2883-2886.

39. Bartolini M, Bertucci C, Bolognesi ML, Cavalli A, Melchiorre C, Andrisano V, Insight into the kinetic of amyloid beta (1–42) peptide self-aggregation: elucidation of inhibitors' mechanism of action, ChemBioChem. 8 (2007) 2152–2161.

40. Miller NJ, Rice-Evans CA. Factors influencing the antioxidant activity determined by the ABTS radical cation assay, Free Radic Res 26. (1997), 195–199.

41. F. Baharloo, MH Moslemin, H. Nadri, A. Asadipour, M. Mahdavi, S. Emami, L. Firoozpour, R. Mohebat, A. Shafiee, A. Foroumadi, Benzofuran-derived benzylpyridinium bromides as potent acetylcholinesterase inhibitors, Eur J Med Chem. 93 (2015) 196–201.

42. BC. Magliaro, CJ. Saldanha, Clozapine protects PC-12 cells from death due to oxidative stress induced by hydrogen peroxide via a cell-type specific mechanism involving inhibition of extracellular signal-regulated kinase phosphorylation, Brain Res. 1283 (2009) 14-24.

43. H. van de Waterbeemd, E. Gifford, ADMET in silico modelling: towards prediction paradise? Nat Rev Drug Discov. 2 (2003) 192-204.

44. http://www.molinspiration.com/services/properties.html

45. W.M. Pardridge, Alzheimer's disease drug development and the problem of the

blood-brain barrier, Alzheimers Dement. 5 (2009) 427-432.

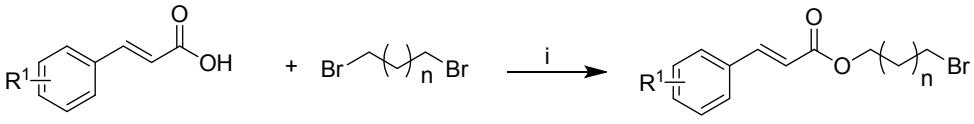

1a-d

1a R^1 = H;
1b R^1 = 3,4-di-OCH_3,;
1c R^1 = 3-OCH_3,4-OH;
1d R^1 = 4-NO_2.

2a-h

2a R^1 = H, n = 0; **2b** R^1 = H, n = 1;
2c R^1 = H, n = 2; **2d** R^1 = H, n = 3;
2e R^1 = H, n = 6; **2f** R^1 = 3,4-di-OCH_3, n = 3;
2g R^1 = 3-OCH_3,4-OH, n = 3; **2h** R^1 = 4-NO_2, n = 3.

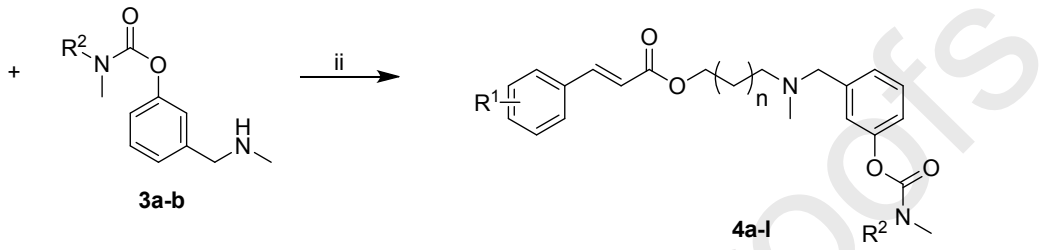

3a-b

4a-l

3a R^2 = CH_3;
3c R^2 = C_2H_5.

4a R^1 = H, R^2 = CH_3, n = 0; **4b** R^1 = H, R^2 = CH_3, n = 1;
4c R^1 = H, R^2 = CH_3, n = 2; **4d** R^1 = H, R^2 = CH_3, n = 3;
4e R^1 = H, R^2 = CH_3, n = 6; **4f** R^1 = 3,4-di-OCH_3, R^2 = CH_3, n = 3;
4g R^1 = 3-OCH_3,4-OH, R^2 = CH_3, n = 3; **4h** R^1 = 4-NO_2, R^2 = CH_3, n = 3;
4i R^1 = H, R^2 = C_2H_5, n = 3; **4j** R^1 = 3,4-di-OCH_3, R^2 = C_2H_5, n = 3;
4k R^1 = 3-OCH_3,4-OH, R^2 =C_2H_5, n = 3; **4l** R^1 = 4-NO_2, R^2 = C_2H_5, n = 3.

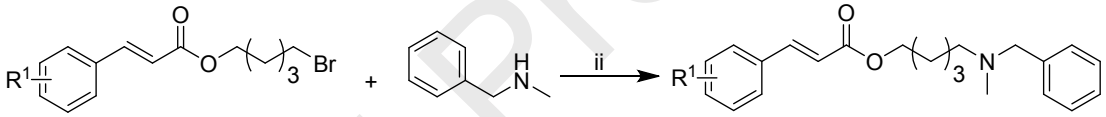

2d/2f-h

3c

4m-o

4m R^1 = H;
4n R^1 = 3,4-di-OCH_3;
4o R^1 = 4-NO_2.

Scheme 1. Synthesis of FA derivatives **4a-o**. Reagents and conditions: (i) Et_3N, acetone, 50 °C., 12 h; (ii) K_2CO_3, CH_3CN, reflux, 12-18 h.

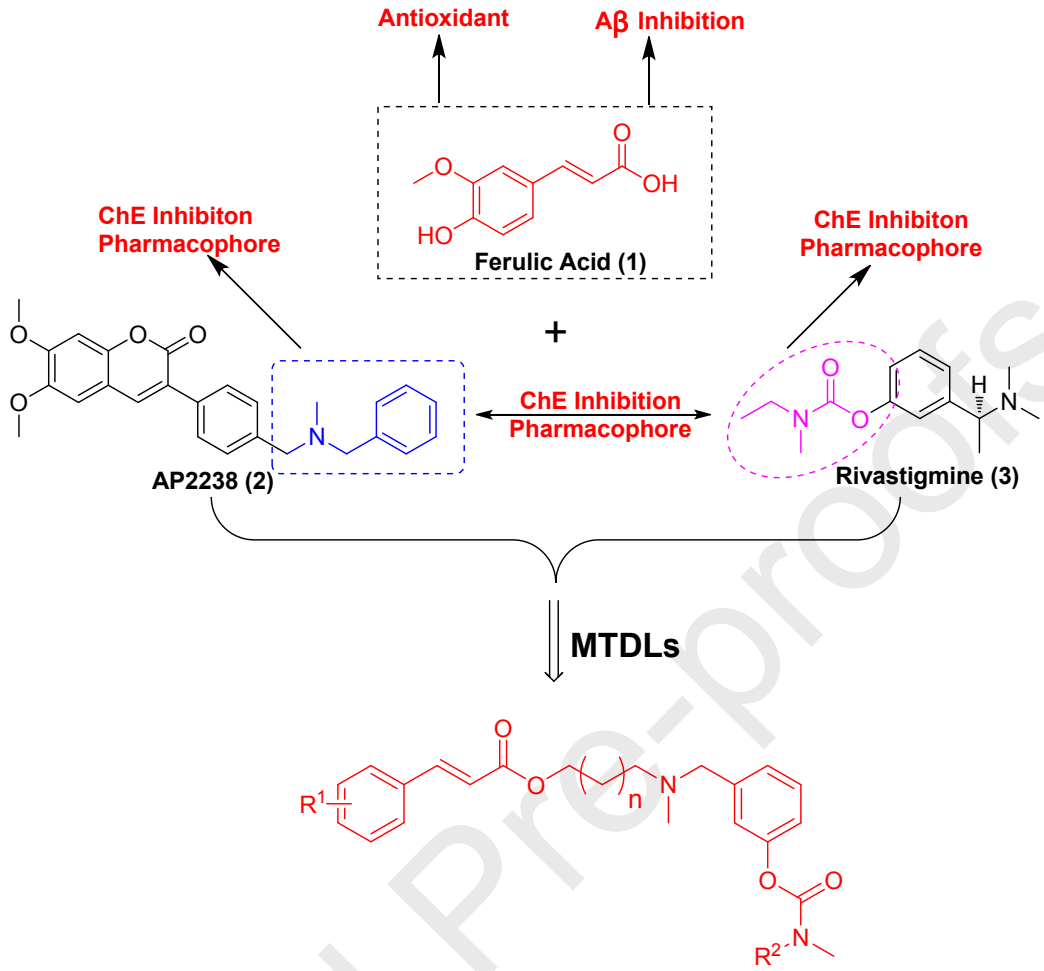

Figure 1. Drug design strategy for multi-target-directed ligands.

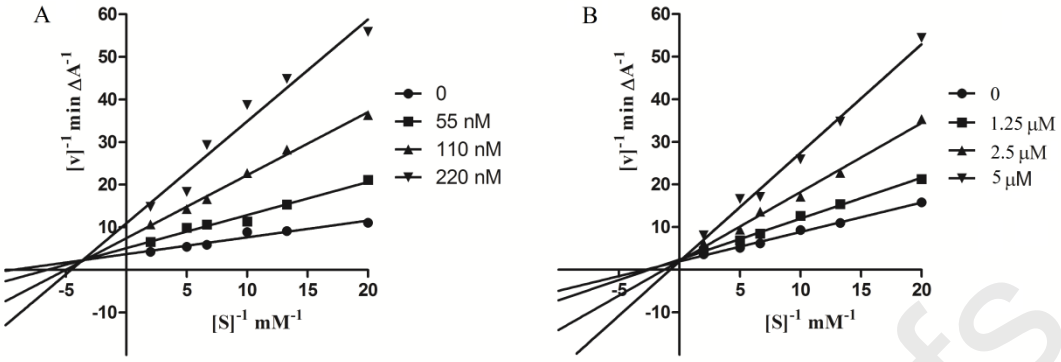

Figure 2. (A) Kinetic study on the mechanism of *Ee*AChE inhibition by compound **4g**. Overlaid Lineweaver–Burk reciprocal plots of AChE initial velocity at increasing substrate concentration (0.05–0.50 mM) in the absence of inhibitor and in the presence of **4g** are shown. (B) Kinetic study on the mechanism of *eq*BuChE inhibition by compound **4g**. Overlaid Lineweaver–Burk reciprocal plots of *eq*BuChE initial velocity at increasing substrate concentration (0.05–0.50 mM) in the absence of inhibitor and in the presence of **4g** are shown. Lines were derived from a weighted least-squares analysis of the data points.

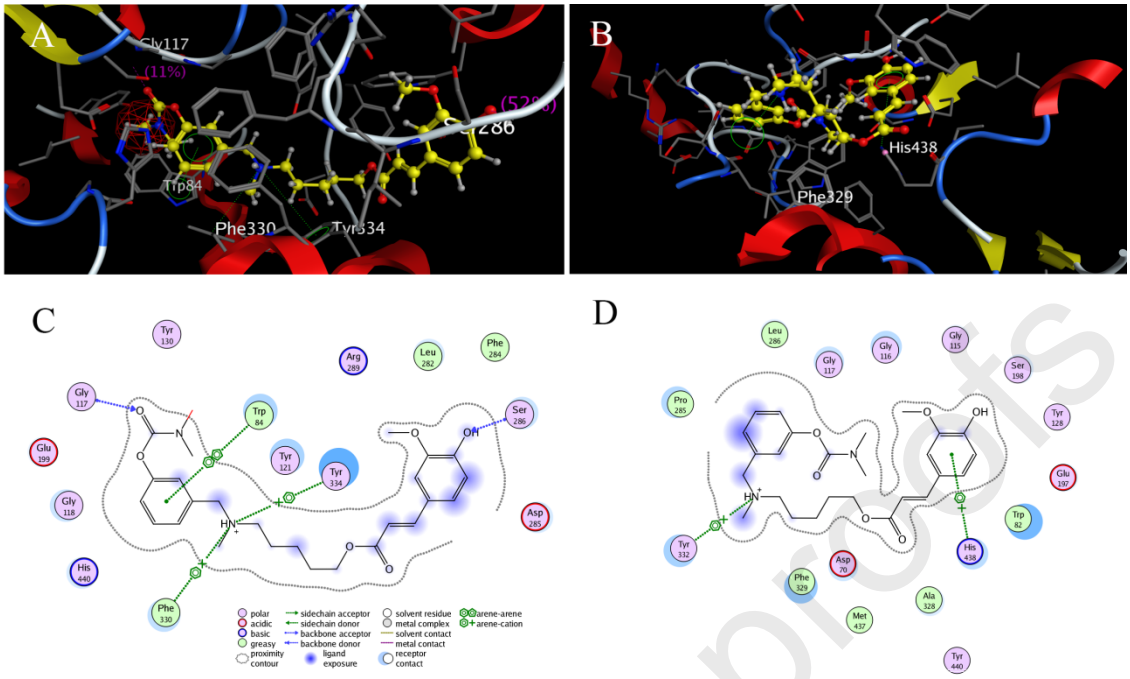

Figure 3. (A) 3D docking model of compound **4g** with *h*AChE. Atom colors: yellow - carbon atoms of **4g**, gray - carbon atoms of residues of *h*AChE, dark blue - nitrogen atoms, red - oxygen atoms. The dashed lines represent the interactions between the protein and the ligand. (B) 3D docking model of compound **4g** with *h*BuChE. Atom colors: yellow - carbon atoms of **4g**, gray - carbon atoms of residues of *h*BuChE, dark blue - nitrogen atoms, red - oxygen atoms. The dashed lines represent the interactions between the protein and the ligand. (C) 2D schematic diagram of docking model of compound **4g** with *h*AChE. (D) 2D schematic diagram of docking model of compound **4g** with *h*BuChE. The figure was prepared using the ligand interactions application in MOE. (For interpretation of the references to color in this figure legend, the reader is referred to the web version of this article.)

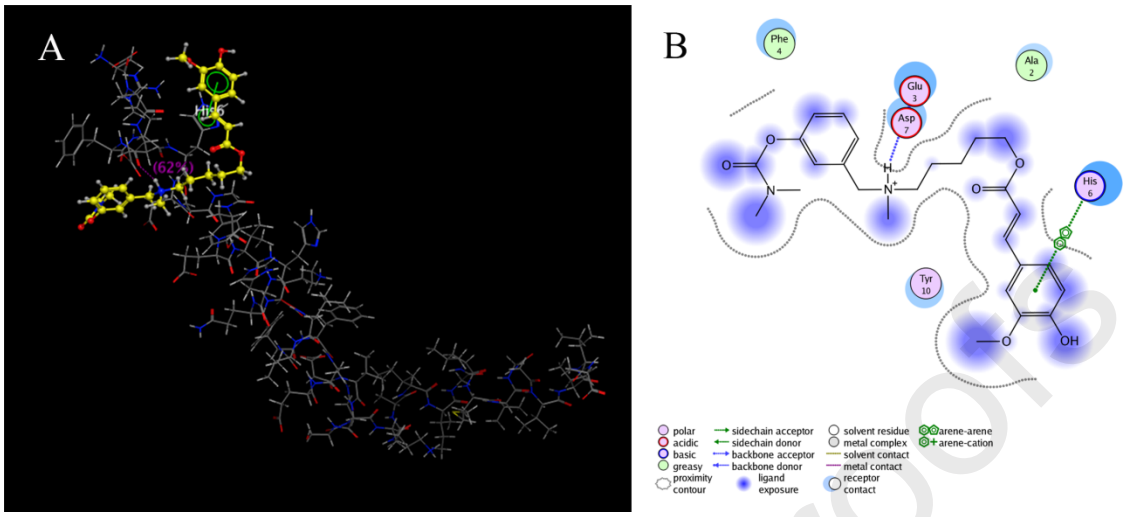

Figure 4. (A) 3D docking model of compound **4g** with Aβ (1-42) generated with MOE. Atom colors: yellow - carbon atoms of **4g**, gray - carbon atoms of residues of Aβ (1-42), dark blue - nitrogen atoms, red - oxygen atoms. The dashed lines represent the interactions between the protein and the ligand. (B) 2D schematic diagram of docking model of compound **4g** with Aβ (1-42).

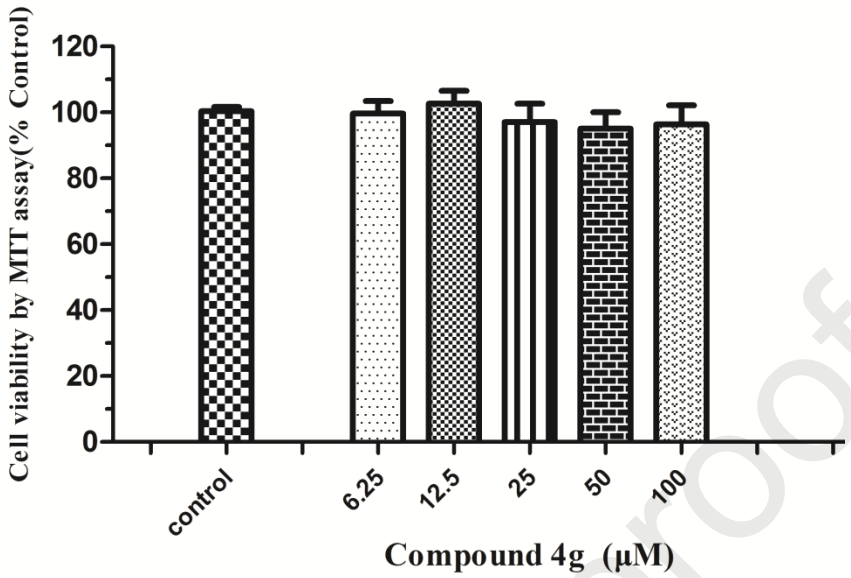

Figure 5. Effects of compound **4g** (6.25-100 μM) on cell viability in PC12 cells. The cell viability was determined by the MTT assay after 24 h of incubation with various concentrations. The results were expressed as a percentage of control cells. Values are reported as the mean ± SD of three independent experiments. Data represent the mean SD of three observations.

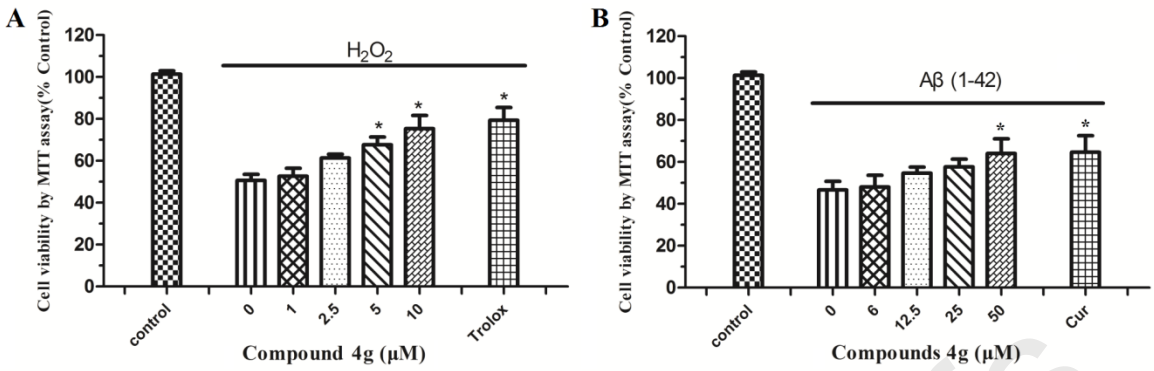

Figure 6. (A) Effect of compound **4g** on H_2O_2-induced oxidative cell damage in PC12 cells. (B) Effect of compound **4g** on Aβ (1-42)-induced cell damage in PC12 cells. Data are means ± SD (n = 5) *$p < 0.05$ compared to the control group.

Table 1. Inhibition of ChEs activity and selectivity index of compounds **4a-o**.

Compound	n	R^1	R^2	IC_{50} (μM) [a]		Selectivity index (SI) [b]
				*ee*AChE	*e*qBuChE	
4a	0	-	CH_3	4.25 ± 0.21	6.32 ± 0.30	1.49
4b	1	-	CH_3	0.77 ± 0.09	8.15 ± 0.13	10.58
4c	2	-	CH_3	0.60 ± 0.04	25.0 ± 0.58	41.67
4d	3	-	CH_3	0.18 ± 0.08	0.84 ± 0.05	4.66
4e	6	-	CH_3	0.44 ± 0.09	10.0 ± 0.14	22.73
4f	3	3,4-di-OCH_3	CH_3	0.086 ± 0.005	1.30 ± 0.03	15.12
4g	3	3-OCH_3,4-OH	CH_3	0.112 ± 0.023	2.44 ± 0.18	21.78
4h	3	4-NO_2	CH_3	0.055 ± 0.008	2.23 ± 0.17	40.55
4i	3	-	C_2H_5	13.28 ± 0.29	1.40 ± 0.08	0.11
4j	3	3,4-di-OCH_3	C_2H_5	5.47 ± 0.22	1.37 ± 0.09	0.25
4k	3	3-OCH_3,4-OH	C_2H_5	9.73 ± 0.19	1.73 ± 0.05	0.18
4l	3	4-NO_2	C_2H_5	19.85 ± 0.28	2.59 ± 0.16	0.13
4m	3	-	-	42.26 ± 0.28	>100	>100
4n	3	3,4-di-OCH_3	-	31.67 ± 0.25	>100	>3.16
4o	3	4-NO_2	-	38.45 ± 0.36	>100	>2.60
Ferulic acid		-	-	>100	>100	-
Donepezil		-	-	0.057 ± 0.006	4.53 ± 0.07	79.47

[a] IC_{50}: 50% inhibitory concentration (means ± SD of three experiments).

[b] Selectivity Index = IC_{50} (*e*qBuChE)/IC_{50} (*ee*AChE).

Table 2. Inhibition of ChEs activity and selectivity index of compounds **4f-h**.

Compounds	IC_{50} [a]		Selectivity Index[b]
	*h*AChE (nM)	*h*BuChE (μM)	
4f	16.5 ± 0.2	0.76 ± 0.03	46.1
4g	19.7 ± 0.4	0.59 ± 0.05	29.9
4h	13.7 ± 0.2	0.66 ± 0.06	48.2
donepezil	30.2 ± 0.8	8.7 ± 0.25	288.1

[a] IC_{50}: 50% inhibitory concentration (means ± SD of three experiments).

[b] Selectivity Index = IC_{50} (*h*BuChE)/IC_{50} (*h*AChE).

Table 3. Inhibition of Aβ (1-42) self-induced aggregation and ABTS radical by target compounds.

Compound	n	R^1	R^2	Aβ(1- 42) aggregation inhibition (%)[a]	ABTS assay (trolox equiv)[b]
4a	0	-	CH_3	38.5 ± 2.5	NT [c]
4b	1	-	CH_3	41.2 ± 1.6	NT
4c	2	-	CH_3	39.7 ± 2.7	NT
4d	3	-	CH_3	40.9 ± 1.8	0.46
4e	6	-	CH_3	41.8 ± 1.9	NT
4f	3	3,4-di-OCH_3	CH_3	49.7 ± 2.3	0.68
4g	3	3-OCH_3,4-OH	CH_3	49.2 ± 1.6	1.26
4h	3	4-NO_2	CH_3	43.5 ± 3.1	0.59
4i	3	-	C_2H_5	43.7 ± 1.9	0.38
4j	3	3,4-di-OCH_3	C_2H_5	51.4 ± 2.5	0.58
4k	3	3-OCH_3,4-OH	C_2H_5	49.9 ± 2.7	1.23
4l	3	4-NO_2	C_2H_5	44.7 ± 1.8	0.55
4m	3	-	-	37.8 ± 2.4	NT
4n	3	3,4-di-OCH_3	-	47.9 ± 2.3	NT
4o	3	4-NO_2	-	42.5 ± 1.8	NT
Ferulic acid	-		-	36.7 ± 2.6	1.12
Curcumin	-		-	58.4 ± 1.9	-

[a] Inhibition of Aβ (1-42) self-induced aggregation, the thioflavin-T fluorescence method was used, the mean ± SD of at least three independent experiments and themeasurements were carried out in the presence of 20 μM compounds.

[b] Data are expressed as (mmol trolox)/(mmol tested compound).

[c] NT. means not test.

Table 4. Some physicochemical parameters of the compounds **4a-o** used in prediction of ADME profiles.

Comp.	MW	logP	tPSA	nON	nOHNH	vol	nrotb	vio
4a	382.46	3.55	59.09	6	0	364.46	10	0
4b	396.49	3.83	59.09	6	0	381.26	11	0
4c	410.51	4.10	59.09	6	0	398.06	12	0
4d	424.54	4.60	59.09	6	0	414.87	13	0
4e	466.62	6.12	59.09	6	0	465.27	16	1
4f	484.59	4.25	77.55	8	0	465.96	15	0
4g	470.57	3.94	88.55	8	1	448.43	14	0
4h	469.54	4.56	104.91	9	0	438.20	14	0
4i	438.57	4.98	59.09	6	0	431.67	14	0
4j	498.62	4.62	77.55	8	0	482.76	16	0
4k	484.59	4.32	88.55	8	1	465.23	15	0
4l	483.59	4.94	104.91	9	0	455.00	15	0
4m	337.46	5.00	29.54	3	0	340.99	11	0
4n	397.51	4.65	48.01	5	0	392.08	13	0
4o	382.46	4.96	75.37	6	0	364.33	12	0
Rules	≤ 450	≤ 5.0	≤ 90	≤ 10	≤ 5	-	-	-

MW: Molecular weight; log P: log octanol/water partition coefficient; tPSA: Total Polar Surface Area; nON: number of Hydrogen acceptors; nOHNH: number of Hydrogen donors; Vol: Molecular volume; nrotb: number of rotatable bonds; log BB = 0.0148 × tPSA + 0.152 × log P + 0.130. Vio: Violation.

Table 5. Permeability ($Pe \times 10^{-6}$ cm s^{-1}) in the PAMPA-BBB assay for 9 commercial drugs, used in the experiment validation.

Commercial drugs	Bibl[a]	PBS:EtOH (70:30)[b]
Testosterone	17	19.39
Verapamil	16	17.18
beta-Estradiol	12	9.28
Progesterone	9.3	7.86
corticosterone	5.1	6.48
Piroxicam	2.5	1.96
Hydrocortisone	1.9	2.56
Ofloxacin	0.8	0.67
Dopamine	0.2	0.15

[a] Taken from Ref.[45]

[b] Data are the mean ± SD of three independent experiments.

Table 6. Permeability ($P_e \times 10^{-6}$cm s^{-1}) in the PAMPA-BBB assay for novel cinnamic acid derivatives and their predictive penetration in the CNS.

Compound	$Pe \times 10^{-6}$cm s^{-1}	Prediction
4f	7.59 ± 0.47	CNS+
4g	6.58 ± 0.32	CNS+

Graphical Abstract

Design, synthesis and evaluation of novel ferulic acid derivatives as multi-target-directed ligands for the treatment of Alzheimer's disease

Jin-Shuai Lan[1,2#], Rui-Feng Zeng[2#], Xiao-Yi Jiang[2], Jian-wei Hou[1], Yun Liu[1], Zheng-Hao Hu[2], Hong-Xin Li[2], Yin Li[4], Sai-Sai Xie[3]*, Yue Ding[1,2]*, Tong Zhang[1,2]*

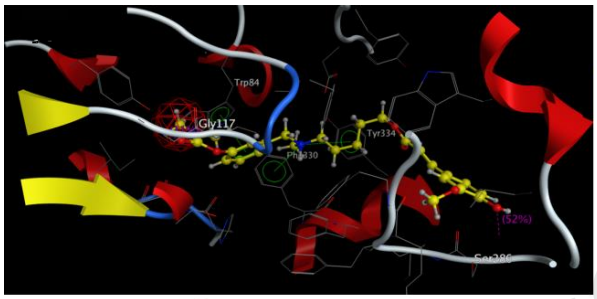

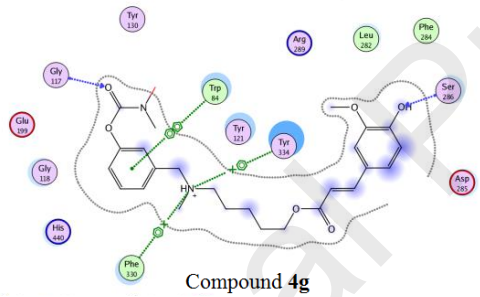

Compound **4g**

- **IC_{50}, 19.7 nM for *h*AChE and 0.66 μM for *h*BuChE**
- **good A*β* aggregation inhibition (49.2% at 20 μM)**
- **good antioxidant activity (1.26 trolox equivalents)**
- **neuroprotection on H_2O_2-induced oxidative cell damage**
- **good BBB permeability by the PAMPA−BBB assay**

Highlights

1. Novel ferulic acid derivatives containing the benzylamino and carbamyl pharmacophores were designed and synthesized.

2. Most compounds were multi-target inhibitors inhibiting cholinesterases (ChEs) and self-induced *β*-amyloid (A*β*) aggregation.

3. Compound **4g** presented the greatest ability to inhibit cholinesterase (IC_{50}, 19.7 nM for *h*AChE and 0.66 μM for *h*BuChE), good A*β* aggregation inhibition (49.2% at 20 μM) and good antioxidant activity (1.26 trolox equivalents).

4. Compound **4g** had neuroprotection on H_2O_2-induced and A*β*-induced PC12 cells damage and could cross the BBB.